

# UC Berkeley

## UC Berkeley Previously Published Works

### Title

Observing ozone chemistry in an occupied residence

### Permalink

<https://escholarship.org/uc/item/2mh6860v>

### Journal

Proceedings of the National Academy of Sciences of the United States of America, 118(6)

### ISSN

0027-8424

### Authors

Liu, Yingjun  
Misztal, Pawel K  
Arata, Caleb  
et al.

### Publication Date

2021-02-09

### DOI

10.1073/pnas.2018140118

Peer reviewed

## Bringing Ozone Chemistry Home

Yingjun Liu<sup>a,b,\*</sup>, Pawel K. Misztal<sup>b,†</sup>, Caleb Arata<sup>c</sup>, Charles J. Weschler<sup>d,e</sup>, William W Nazaroff<sup>f</sup>,  
and Allen H. Goldstein<sup>b,f</sup>

<sup>a</sup> BIC-ESAT and SKL-ESPC, College of Environmental Sciences and Engineering, Peking University, Beijing 100871, China;

<sup>b</sup> Department of Environmental Science, Policy, and Management, University of California, Berkeley, CA 94720;

<sup>c</sup> Department of Chemistry, University of California, Berkeley, CA 94720;

<sup>d</sup> Environmental and Occupational Health Sciences Institute, Rutgers University, Piscataway, NJ 08854;

<sup>e</sup> International Centre for Indoor Environment and Energy, Technical University of Denmark, Lyngby 2800, Denmark;

<sup>f</sup> Department of Civil and Environmental Engineering, University of California, Berkeley, CA 94720;

<sup>†</sup> Now at Civil, Architectural and Environmental Engineering, University of Texas at Austin, Austin, TX 78712.

\* Correspondence: Yingjun Liu. *E-mail:* [yingjun.liu@pku.edu.cn](mailto:yingjun.liu@pku.edu.cn); *Tel:* 86-10-6275572.

Submitted September 2020; revised November 2020

*Proceedings of the National Academy of Sciences of the U.S.A.*

**Classification:** Physical Sciences/Environmental Sciences

**Key words:** ozonolysis; indoor; residential; ventilation; squalene; exposure

## 1 **Abstract**

2 Outdoor ozone transported indoors initiates oxidative chemistry, forming volatile organic  
3 products. The influence of ozone chemistry on indoor air composition has not been directly  
4 quantified in normally occupied residences. Here, we explore indoor ozone chemistry in a house  
5 in California with two adult inhabitants. We utilize space- and time-resolved measurements of  
6 ozone and volatile organic compounds (VOCs) acquired over an eight-week summer campaign.  
7 Despite overall low indoor ozone concentrations (mean value of 4.3 ppb) and a relatively low  
8 indoor ozone decay constant ( $1.3 \text{ h}^{-1}$ ), we identified multiple VOCs exhibiting clear contributions  
9 from ozone-initiated chemistry indoors. These chemicals include 6-methyl-5-hepten-2-one (6-  
10 MHO), 4-oxopentanal (4-OPA), nonenal, and C8-C12 saturated aldehydes, which are among the  
11 commonly reported products from laboratory studies of ozone interactions with indoor surfaces  
12 and with human skin lipids. These VOCs together accounted for  $\geq 12\%$  molecular yield with  
13 respect to house-wide consumed ozone, with the highest net product yields for nonenal ( $\geq$   
14 3.5%), followed by 6-MHO (2.7%) and 4-OPA (2.6%). Although 6-MHO and 4-OPA are  
15 prominent ozonolysis products of skin lipids (specifically squalene), ozone reaction with the  
16 body envelopes of the two occupants in this house are insufficient to explain the observed yields.  
17 Relatedly, we observed that ozone-driven chemistry continued to produce 6-MHO and 4-OPA  
18 even after the occupants had been away from the house for 5 days. These observations provide  
19 evidence that skin lipids transferred to indoor surfaces made substantial contributions to ozone  
20 reactivity in the studied house.

21 **Significance Statement**

22           It has been suggested that indoor exposure to ozone oxidation products contributes  
23 materially to the apparent associations between outdoor ozone concentration and morbidity and  
24 mortality. Our current understanding of indoor ozone chemistry derives mainly from studies  
25 with test surfaces under controlled conditions. Little is known about the overall impact of ozone  
26 chemistry on air composition in dynamically changing indoor residential environments. The  
27 results presented here reflect the first quantitative characterization of overall indoor ozone  
28 chemistry in a normally occupied home. Findings reveal a strong influence of off-body skin  
29 lipids on indoor ozone chemistry. Being able to elucidate indoor air pollutants derived from  
30 ozone chemistry facilitates the investigation of causal links between outdoor ozone  
31 concentrations and adverse health effects.

## 32 **Main Text**

### 33 **Introduction**

34 Outdoor air containing ozone (O<sub>3</sub>) penetrates into indoor environments, including  
35 residences, workplaces, and schools. Ozone undergoes fast reactions indoors; its characteristic  
36 lifetime is typically a few tens of minutes (1, 2). Reactions are thought mainly to occur on the  
37 large surface area in indoor environments (3), which ubiquitously contain reactive species (4, 5).  
38 Indoor ozone chemistry reduces indoor ozone concentrations and forms a spectrum of oxidation  
39 products, many of which are volatile (6). Emerging evidence suggests that indoor exposure to  
40 the mixture of ozone and its oxidation products contributes to epidemiologically determined  
41 associations between outdoor ozone concentrations and morbidity and mortality (3, 7).

42 Previous studies of indoor air chemistry mainly focused on investigating ozone reactions  
43 with individual indoor surfaces along with consequent release of secondary products. Studied  
44 surfaces include building materials and furnishings, such as carpet, wall covering, ceiling tile,  
45 wood board, and glass (8–11), as well as human skin, hair, and clothing (12–14). Observed  
46 volatile products include C1-C13 carbonyls, dicarbonyls, and hydroxycarbonyls among other  
47 oxygenated compounds. Product yields vary broadly, influenced by factors such as type and age  
48 of surface materials (11, 15) and soiling (8, 13, 16, 17). Skin oil lipids, characterized by a high  
49 proportion of squalene (C<sub>30</sub>H<sub>50</sub>), are particularly important indoor ozone reactants (14). They are  
50 present on skin, hair, and worn clothing of human occupants. They can also be transferred to  
51 other surfaces such as bedding, furniture, and flooring via desquamation and by direct physical  
52 contact (18). Major volatile products of squalene ozonolysis include 4-oxopentanal (4-OPA), 6-  
53 methyl-5-hepten-2-one (6-MHO), and geranylacetone.

54 Past research targeting specific indoor materials and surfaces demonstrates important  
55 features of indoor surface ozone chemistry; however, these studies are insufficient for evaluating

56 the contribution of ozone chemistry to the composition of dynamically changing indoor  
57 environments and hence to occupants' exposure (19). First, there can be myriad sources for  
58 indoor air pollutants in addition to ozone chemistry (20). Because ozone chemistry can produce  
59 a particular compound does not imply that it contributes meaningfully to the indoor  
60 concentration of that compound. Second, occupants might dynamically alter indoor ozone  
61 reactivity via their time-dependent presence indoors as well as their intended and unintended  
62 activities such as desquamation, transferring skin oils to surfaces by direct contact, cooking (e.g.,  
63 surface soiling by the deposition of fatty acids in cooking oils and foods), and cleaning (e.g.,  
64 with products that contain ozone-reactive terpenoids). Indoor studies in densely occupied spaces,  
65 including in two classrooms, a simulated office, and a simulated aircraft cabin (14, 21–23), have  
66 all highlighted the importance of the direct presence of human occupants for ozone chemistry.  
67 For residences, which are often less densely occupied, evidence is lacking regarding the overall  
68 features of indoor ozone chemistry and its impact on the indoor air composition to which  
69 occupants are exposed.

70 Here, we report an investigation of indoor ozone chemistry in a normally occupied  
71 residence based on temporally and spatially resolved observations of volatile organic compounds  
72 (VOCs) and ozone. Data were acquired in a single-family house in Oakland, California, from an  
73 extensive eight-week monitoring campaign conducted during summer 2016 (24, 25). This paper  
74 builds on our earlier analysis of the same data set regarding ventilation and airflow patterns in  
75 the house (25), as well as concentrations and source characteristics of indoor VOCs (24). In this  
76 paper, we examine the spatial and temporal distribution of ozone concentration, estimate the  
77 chemical loss rate coefficient of ozone in the living space, characterize the oxidation products of  
78 skin oil lipids, and undertake a non-targeted analysis to identify VOC species significantly  
79 derived from ozone-initiated chemistry.

## 80 **Results and Discussion**

81 **Ozone in the house.** Figure 1 (top) presents the diel variation of ozone concentration  
82 measured at different locations in the house during the occupied period under the space-resolved  
83 measurement scheme (cf. Materials and Methods). Mean ozone mixing ratios during the same  
84 periods are reported in Table 1. The outdoor ozone level exhibited modest diel variation, with  
85 the hourly median peaking at 28 ppb in the afternoon and declining to 20 ppb in the early  
86 morning. The ozone level in different compartments of the house can be understood in the  
87 context of the airflow patterns, i.e., with air generally flowing upwards from the crawlspace to  
88 the living space and then to the attic; downwards flows were rare (25). The crawlspace air,  
89 coming directly from outdoors through designed vents, exhibited consistently low ozone levels  
90 (a mean value of 3.4 ppb), indicating substantial ozone loss in the crawlspace. The loss may be  
91 associated with ozone titration by NO emitted from pilot lights of one or both of the natural-gas  
92 furnace and water heater installed in the crawlspace; elevated NO was observed in the  
93 crawlspace during wintertime monitoring in this house (26). The airflow path into the living  
94 space showed a strong diel variation, with 90% of air infiltrating from the ozone-deficient  
95 crawlspace at night whereas 80% directly entered from outdoors in the afternoon through opened  
96 windows (Fig. 1 bottom). Correspondingly, the median indoor-to-outdoor (I/O) ratio of ozone  
97 varied from 0.12 at night to ~ 0.27 in the afternoon (Fig. 1 middle). As a point of comparison,  
98 previously reported I/O ratios for ozone are typically in the range 0.2 - 0.7 (6). In the  
99 unoccupied (and unfinished) attic, where airflow originated both from the living space and from  
100 outdoors, the ozone level was similar to that in the living space, whereas in the small basement  
101 room, with a constantly open window, ozone exhibited strong diel variation that was closest to  
102 outdoor concentrations in the mid-afternoon.

103 The following analysis mainly focuses on the living space where human exposure occurs.  
 104 The mean ozone level in the living space (indoor ozone) was only 4.3 ppb, at the lower end of  
 105 reported values for residences in California (27). Assuming a well-mixed living space, the  
 106 indoor ozone concentration  $[O_3]_{in}$  is described well by the following equation

$$107 \quad \frac{d[O_3]_{in}}{dt} = (f_{crawl}[O_3]_{crawl} + f_{out}[O_3]_{out})ACR - (ACR + k_{O_3})[O_3]_{in}, \quad (1)$$

108 where  $[O_3]_{crawl}$  and  $[O_3]_{out}$  are the ozone concentrations (ppb) measured in the crawlspace and  
 109 outdoors respectively;  $f_{crawl}$  and  $f_{out}$  are the fraction of airflow into the living space from the  
 110 crawlspace and outdoors, respectively;  $ACR$  is the air change rate of the living space ( $h^{-1}$ ), and  
 111  $k_{O_3}$  is the first-order chemical loss rate coefficient of ozone in the living space ( $h^{-1}$ ). In Eq. 1,  
 112 ozone loss across the building envelope through intended and unintended openings is neglected  
 113 (28). Rearranging Eq. 1, we can estimate the overall chemical loss rates of ozone  $L_{O_3}$  (ppb/h) as  
 114 follows:

$$115 \quad L_{O_3} = k_{O_3}[O_3]_{in} = (f_{crawl}[O_3]_{crawl} + f_{out}[O_3]_{out} - [O_3]_{in})ACR - \frac{d[O_3]_{in}}{dt}. \quad (2)$$

116 For use of Eq. 2,  $ACR$ ,  $f_{crawl}$ , and  $f_{out}$  were calculated with 2-h resolution, utilizing tracer-gas  
 117 measurements to determine time-resolved air change rate (25).

118 The indoor ozone chemical loss rate,  $L_{O_3}$ , with 2-h resolution, was obtained for all space-  
 119 resolved measurement periods. Figure 2 shows the scatter plot of  $L_{O_3}$  versus the ozone  
 120 concentration  $[O_3]_{in}$  in the living space. Given the low ozone level in the crawlspace, data are  
 121 only shown for  $f_{out} > 0.6$  to exclude low-signal values with correspondingly high uncertainty, and  
 122 thus emphasizing daytime data. In Fig. 2, the slope from any data point to zero would  
 123 correspond to its  $k_{O_3}$  value ( $k_{O_3} = L_{O_3} / [O_3]_{in}$ ). As shown in Fig. 2,  $k_{O_3}$  values of most data  
 124 points lie within lines corresponding to the range  $0.8-2.0 h^{-1}$ , and the overall best-fit  $k_{O_3}$  value is



125  $1.3 \text{ h}^{-1}$ . These values are at the lower end of reported ozone decay rate coefficients in residences.  
126 For example, measured  $k_{\text{O}_3}$  values varied from  $1 \text{ h}^{-1}$  to  $8 \text{ h}^{-1}$  in 43 homes in South California with  
127 mean ( $\pm$  SD) of  $2.8 (\pm 1.3) \text{ h}^{-1}$  (2), and varied from  $1.3 \text{ h}^{-1}$  to  $6.0 \text{ h}^{-1}$  in 14 residences in China (1).  
128 Note that our results were obtained under normal occupancy without manipulating indoor ozone,  
129 whereas the cited studies derived  $k_{\text{O}_3}$  by experimentally elevating ozone and then monitoring its  
130 decay under house-closed condition in the absence of occupants. The sustained long-term  
131 average ozone loss rate (as measured in our work) might be lower than the short-term loss rate  
132 associated with a sudden ozone enhancement (as reported in prior literature).

133 **Ozonolysis products from squalene.** Next, we explore the VOC data for products  
134 arising from indoor ozonolysis. VOC signals were measured using a proton-transfer-reaction  
135 time-of-flight mass spectrometer (PTR-ToF-MS; see Materials and Methods). Our analysis  
136 starts by focusing on the unique and most abundant volatile products of squalene ozonolysis: 6-  
137 MHO ( $\text{C}_8\text{H}_{14}\text{O}$ ) and 4-OPA ( $\text{C}_5\text{H}_8\text{O}_2$ ). In PTR-MS analysis, 6-MHO is detected as  $\text{C}_8\text{H}_{15}\text{O}^+$  and  
138  $\text{C}_8\text{H}_{13}^+$  ions and 4-OPA appears as the  $\text{C}_5\text{H}_9\text{O}_2^+$  ion (22). Measured signals of these ions might  
139 also have contribution from other isomeric compounds. Below we show that the temporal  
140 pattern of indoor  $\text{C}_8\text{H}_{15}\text{O}^+$  and  $\text{C}_5\text{H}_9\text{O}_2^+$  signals is consistent with the dominant contribution  
141 originating from 6-MHO and 4-OPA.

142 Figure 3 shows a one-week time series of  $\text{C}_8\text{H}_{15}\text{O}^+$  and  $\text{C}_5\text{H}_9\text{O}_2^+$  ions, as well as time  
143 series of factors that possibly influence indoor 6-MHO and 4-OPA, including occupancy, air  
144 change rates, indoor temperature, and indoor ozone concentration. Signals of both  $\text{C}_8\text{H}_{15}\text{O}^+$  and  
145  $\text{C}_5\text{H}_9\text{O}_2^+$  ions in the kitchen and bedroom were more than an order of magnitude higher than  
146 outdoors, indicating strong indoor sources. A key feature of the time series is that higher indoor  
147 signals were typically observed during daytime when the air change rates and indoor ozone  
148 concentrations were higher (e.g., September 20-24). Higher air change rate alone is normally

149 expected to reduce indoor concentration of species with a dominant indoor source. The higher  
150 ion signals of  $C_8H_{15}O^+$  and  $C_5H_9O_2^+$  observed in these cases is consistent with theoretical  
151 predictions that 6-MHO and 4-OPA production from squalene ozonolysis can outweigh removal  
152 by ventilation (29). In particular, when the occupants hosted a party on the evening of 22  
153 September, with 17 persons present in the house (and, therefore, substantially more squalene  
154 available for ozonolysis), elevated  $C_8H_{15}O^+$  and  $C_5H_9O_2^+$  signals were observed despite the  
155 higher ventilation rate during that event. Additionally, signals of the two ions exhibited sporadic  
156 and brief spikes, likely associated with sources other than squalene ozonolysis or other  
157 compounds (SI Appendix). However, these spikes only represent minor contributions to overall  
158 ion signals.

159 Further analysis is based on net indoor source strengths ( $S$ ) of VOC signals instead of  
160 their concentrations. Utilizing a mass-balance equation, indoor source strengths of VOC signals  
161 (ppb/h) have been determined with 2-h resolution from simultaneously measured air change rates  
162 and indoor and outdoor concentrations (24). If the indoor source strength ( $S_i$ ) of a VOC  $i$  is  
163 contributed by production ( $P_i$ ) from ozone chemistry, in addition to direct emission, one can  
164 represent the total production rate as  $S_i = S_{i,0} + P_i = S_{i,0} + k_i [O_3]_{in}$ , where  $S_{i,0}$  is the ozone-  
165 independent emission rate of  $i$  (ppb/h); and  $k_i$  is an effective first-order production rate  
166 coefficient of  $i$  from ozone reaction ( $h^{-1}$ ). In the case that squalene ozonolysis is the dominant  
167 reaction to produce  $i$ ,  $k_i$  would be proportional to the amount of squalene indoors available for  
168 reaction. Note that this equation is a simplified representation; the determined  $S_i$  is a net value,  
169 incorporating not only indoor emission and chemical production, but also indoor wall interaction  
170 and possible indoor loss from chemical reaction.

171 Figure 4A shows the dependence of source strength of the  $C_8H_{15}O^+$  ion on indoor ozone  
172 concentration  $[O_3]_{in}$  with data points colored by occupancy. Figure 4A includes all available

173 data subject to the constraint that indoor temperature is restricted to the range 20.5-23.5 °C to  
174 minimize possible confounding effects of temperature (Fig. S1). As shown in Fig. 4A,  $C_8H_{15}O^+$   
175 source strength exhibits close correlation with indoor ozone. The  $R^2$  of a linear fit of the data set  
176 after excluding two outliers (source strength greater than upper quartile plus  $3\times$  interquartile  
177 range) is 0.66. The fitted slope, corresponding to the production rate coefficient of  $C_8H_{15}O^+$   
178 from first-order ozone reaction ( $k$ ), is  $0.018\text{ h}^{-1}$ . The fitted intercept, corresponding to ozone-  
179 independent baseline emission rate ( $S_0$ ), is  $0.0072\text{ ppb/h}$ . A striking feature in Figure 4A is that  
180 the baseline emission  $S_0$  (intercept) was small compared with the range of ozone-dependent  
181 production  $k[O_3]_{in}$  (e.g., an increase by  $0.18\text{ ppb/h}$  for  $10\text{ ppb}$  of indoor ozone). This feature  
182 quantitatively demonstrates that 6-MHO production from ozone chemistry was the dominant  
183 source of measured  $C_8H_{15}O^+$  signals. A similarly strong dependence of source strength on ozone  
184 was also found for  $C_8H_{13}^+$  (the other product ion of 6-MHO) and  $C_5H_9O_2^+$  (4-OPA), as presented  
185 in Figure S2.

186 Figure 4A also explores the role of occupancy. Since only two adults lived in the house,  
187 two or fewer persons were typically present in the living space, with some exceptions due to  
188 visits of guests (particularly during the party). Data for the presence of more than 4 persons are  
189 labeled in Fig. 4A. Although there were only four such points, they each lie above the general  
190 trend line. Such occupancy dependence is consistent with expectations for squalene ozonolysis:  
191 more people present in the house would mean more squalene available for ozone reaction,  
192 leading to a larger  $k$  value. The role of occupancy is also evident in the spatial distribution of  
193 ozone oxidation products associated with squalene. Table 1 shows that ions associated with 6-  
194 MHO and 4-OPA were much higher in the routinely occupied spaces (kitchen and bedroom) than  
195 in rarely occupied auxiliary spaces (crawl space and attic). Given the regular movement of air  
196 from the kitchen and bedroom to attic, it is reasonable that the concentrations in the attic were

197 higher than those in the crawlspace. A comparison of basement and crawlspace levels is also  
198 informative. The basement exhibited the highest level of ozone (Fig. 1) and also was a site for a  
199 clothes washer and soiled laundry; the crawlspace was never occupied and did not contain  
200 clothing or other objects associated with occupant contact. The  $C_8H_{15}O^+$  signal was much higher  
201 in the basement than in the crawlspace.

202 Figure 4B explores the role of occupancy for cases with a low occupancy level by  
203 analyzing a subset of data from Figure 4A with indoor ozone concentration restricted to the  
204 range 2-4 ppb. This ozone range was chosen because it covered most data points during periods  
205 with zero occupancy. Figure 4B plots the source strength of  $C_8H_{15}O^+$  signals as a function of  
206 occupancy (left frame for  $0 < \text{occupancy} \leq 2$  persons) and then the elapsed time since the house  
207 was last occupied (right frame for occupancy = 0). From the left frame, one cannot clearly  
208 discern how  $C_8H_{15}O^+$  source strength changed with occupancy level given the variability of the  
209 data. For periods with between one and two occupants, the source strength averaged 0.056 ppb/h  
210 with a standard deviation of 0.014 ppb/h. However, when the house was unoccupied (right  
211 frame),  $C_8H_{15}O^+$  source strength slowly decreased with the duration of vacancy. The source  
212 strength was about  $0.045 \pm 0.016$  ppb/h when the house was unoccupied for less than 1 h and  
213 diminished by about half, to  $0.023 \pm 0.003$  ppb/h, when the unoccupied period of time increased  
214 to ~130 h. Given that the reaction between ozone and 6-MHO is fast (second-order rate  
215 coefficient of  $3.9 \times 10^{-16} \text{ cm}^3 \text{ mol}^{-1} \text{ s}^{-1}$  (30)), along with the small intercept in Figure 4a (baseline  
216 emission level of 0.007 ppb/h), it is unlikely that surface reservoirs were a substantial source of  
217 6-MHO during the unoccupied period. Instead, the more probable explanation is that ozone  
218 reacted with squalene in skin flakes and skin oils that had accumulated on exposed surfaces in  
219 the home. Assuming that this interpretation is correct, we can further infer that during normal  
220 occupancy (Fig. 4B Left) the contribution of off-body skin oil/flakes to  $C_8H_{15}O^+$  source strength

221 (~ 0.045 ppb/h, estimated as the level during initial unoccupied period) was substantially larger  
222 than the contribution from the body envelopes of the occupants (~ 0.011 ppb/h, estimated as the  
223 difference of 0.056 ppb/h and 0.045 ppb/h).

224 This evidence contains a clue to help reconcile the apparent contradiction between the  
225 elevation of  $C_8H_{15}O^+$  source strength in the presence of > 4 persons (Fig. 4A) and the absence of  
226 any source-strength dependence on occupancy level under the normally low occupancy (Fig. 4B  
227 Left). That is, the off-body squalene contributes substantially to the total squalene-associated  
228 ozone reactivity when the house is normally occupied by 2 (or fewer) occupants, such that the  
229 influence of occupancy changes is attenuated. With this interpretation, the contribution of on-  
230 body squalene became substantial only in the rare presence (during this monitoring campaign) of  
231 multiple guests.

232 The large contribution of off-body skin oils is also consistent with high effective yields of  
233 6-MHO and 4-OPA in this study. The effective yields of 6-MHO and 4-OPA (Table 1) were  
234 estimated by taking the ratio of (a) the total production rate coefficient  $\sum k_i$  of corresponding  
235 identified VOC signals (slope in Fig. 4A and Fig. S2) to the chemical loss-rate coefficient of  
236 ozone,  $k_{O_3}$  (Fig. 2), i.e.,  $y_i = \sum k_i / k_{O_3}$ . By definition, the obtained effective yields are relative to  
237 the total ozone loss in the house on a molecular basis and provide overall characterization of  
238 indoor ozone chemistry without differentiating among organic/inorganic precursors,  
239 primary/secondary reactions, or heterogeneous/gas-phase reactions. That said, we expect most  
240 surfaces to be covered with thin films that result from the accumulation over time of semivolatile  
241 organic compounds and airborne particles (4, 31, 32). The house where the sampling occurred  
242 was built in the 1930s and there had been no recent renovation or refurbishing of note. As has  
243 been demonstrated for freshly cleaned windows (33) and vertically positioned glass capillary  
244 tubes (34), organic surface films with thickness on the order of 10 to 20 nm accumulate over

245 months in typical indoor environments. In the studied house of volume 350 m<sup>3</sup> (floor area ~ 140  
246 m<sup>2</sup>) normally occupied by two adults, the combined effective yield of 6-MHO and 4-OPA was  
247 5.2% per consumed ozone, on a molecule-by-molecule basis. Remarkably, this combined yield  
248 is as high as that reported for a simulated aircraft cabin of 28.4 m<sup>3</sup> in the presence of 16 subjects  
249 (22). The simulated aircraft was only occupied during the experiments and was unlikely to have  
250 been widely soiled with skin flakes and skin oils to the extent that an occupied home would be.  
251 Although other factors might also come into play, substantial soiling by skin flakes and skin oil  
252 could help reconcile the observed high yield of squalene oxidation products despite the low  
253 occupant density in this study.

254 A contribution to ozone reactivity from off-body skin flakes/oil has been anticipated (18,  
255 35) and is supported by recent studies (4, 32). The magnitude of this contribution compared to  
256 that of on-body squalene revealed herein is potentially surprising. However, upon closer  
257 examination the result seems reasonable. Two humans in 350 m<sup>3</sup> of living space are estimated to  
258 remove ozone with a first-order rate constants of ~ 0.2 h<sup>-1</sup> (18), which accounted for about one-  
259 sixth the central tendency for  $k_{O_3}$  in Figure 2 (1.3 h<sup>-1</sup>). While we do not know the contribution to  
260  $k_{O_3}$  of skin flakes and skin oils accumulated on “off-body” surfaces, circumstantial evidence  
261 indicates that it is significant. Humans shed their entire outer layer of skin every 2–4 weeks (36).  
262 In dust samples collected from 500 children’s bedrooms in Odense, Denmark, squalene was the  
263 third most abundant identified organic, with a median mass fraction of 32 µg/g (35). Squalene is  
264 semivolatile, with a vapor pressure of  $3.7 \times 10^{-7}$  Pa at 25 °C (37), and so sorption to indoor  
265 surfaces via gas-phase transport may also occur. Furthermore, the low level of indoor ozone at  
266 the residence that we studied might contribute to the accumulation of off-body squalene since the  
267 persistence time scale of squalene should be longer with slower ozonolysis. As a related point,  
268 Deming and Ziemann recently reported an observation of ubiquitous C=C bonds in surface films

269 on various indoor surfaces in a classroom and proposed that human skin lipids could be a major  
270 source (4). Based on decrease of 6-MHO source strength during the vacant period, we roughly  
271 estimated the lifetime of off-body squalene was ~400 h and the total amount of off-body  
272 squalene present was ~0.36 mmol (equal to 150 mg) (SI Appendix). The associated surface C=C  
273 concentration would be ~ 2  $\mu\text{mol}/\text{m}^2$ , largely consistent with the observations of Deming and  
274 Ziemann (4).

275 Previous indoor studies in simulated microenvironments as well as a classroom have  
276 highlighted the importance of ozone reactions with on-body squalene (14, 21, 22). The current  
277 finding identifies a substantial contribution of off-body skin lipids to ozone chemistry in a  
278 normally occupied residence. The new information about factors that can materially influence  
279 exposure to ozone and its byproducts merits further investigation. Contributions of off-body skin  
280 oils might also influence densely occupied environments, in addition to residences. For example,  
281 Tang et al. estimated occupant and non-occupant VOC source strengths in a university classroom  
282 in California (38). Their results indicated a non-occupant source strength of about 25% of the  
283 occupant source for 6-MHO, and about 80% for 4-OPA. It is plausible that these contributions  
284 resulted from ozonolysis of off-body squalene that originated from skin oils and skin flakes of  
285 classroom occupants. Additionally, our results call for caution in extrapolating simulated  
286 scenarios of ozone chemistry in test houses or chambers. That is, because such facilities are not  
287 routinely occupied, they lack an important element of real-world settings – soiling of indoor  
288 surfaces by the skin oil and skin flakes of occupants.

289 **Non-targeted analysis of ozonolysis products.** To explore whether other indoor VOCs  
290 might be substantially associated with ozonolysis, we developed and applied a systematic  
291 screening approach. As a screening index, we computed a dimensionless source strength ratio,  
292 defined as the increase in source strength for a fixed increment (10 ppb) of ozone concentration

293 ( $\Delta S_{10 \text{ ppb O}_3}$ ) divided by the baseline source strength ( $S_0$ ). A higher value of  $\Delta S_{10 \text{ ppb O}_3} / S_0$   
294 indicates a larger contribution of ozone chemistry to the overall VOC signal. As illustrated in  
295 Fig. 4A, this index can be obtained from the linear fit of indoor source strength of a VOC signal  
296 versus indoor ozone over a restricted indoor temperature range (20.5-23.5 °C) and after  
297 removing extreme outliers, where  $S_0$  corresponds to the fitted intercept and  $\Delta S_{10 \text{ ppb O}_3}$  is extracted  
298 from the fitted slope.

299 A confounding factor in the evaluation of this index is ventilation. Due to effects of  
300 indoor surface reservoirs, an increase of ventilation rate was associated with a less-than-  
301 anticipated decrease of indoor VOC signals (39, 40), and, hence, an apparent increase of net  
302 source strength (Fig. S3). Considering that indoor ozone levels tended to be higher with higher  
303 ventilation rates (Fig. 3), this effect can create a correlation between indoor source strength and  
304 ozone, even for compounds whose constituents do not have oxygen and therefore clearly did not  
305 arise directly from ozonolysis (Fig. S3). To compensate, we compute a supplementary index, the  
306 concentration ratio of a species at two air change rates —  $1 \text{ h}^{-1}$  and  $0.25 \text{ h}^{-1}$  ( $C_{1 \text{ h}^{-1}} / C_{0.25 \text{ h}^{-1}}$ ) —  
307 which is an indicator of the surface-reservoir effect. Values of this index for VOC signals were  
308 obtained from linear fits of indoor-outdoor concentration difference versus air change rate at  
309 20.5-23.5 °C, after removing outliers.

310 Figure 5 shows a scatter plot of  $\Delta S_{10 \text{ ppb O}_3} / S_0$  versus  $C_{1 \text{ h}^{-1}} / C_{0.25 \text{ h}^{-1}}$  for 61 VOC signals  
311 that feature continuous indoor sources. These signals were selected based on the same criteria as  
312 in our previous paper, excluding those that have either strong influence from intermittent  
313 emissions (such as cooking) or considerable contributions from outdoors or crawlspace air (24).  
314 Each data point represents a VOC signal. The color indicates the  $R^2$  of the linear fit of its source  
315 strength versus indoor ozone. The point size scales with the fitted slope. Values of  $C_{1 \text{ h}^{-1}} / C_{0.25 \text{ h}^{-1}}$   
316 ranged from 0.45 to 1.37, much higher than the value of 0.25 that would be expected for a



317 constant source strength case, with no wall effects, and for steady-state conditions. Values of  
318  $\Delta S_{10 \text{ ppb O}_3} / S_0$  ranged from 0.6 to 26.

319 Most data points in Fig. 5 are distributed along a line with a positive slope; other points  
320 lie above the line. The line represents a lower bound of  $\Delta S_{10 \text{ ppb O}_3} / S_0$  for a given  $C_{1 \text{ h}^{-1}} / C_{0.25 \text{ h}^{-1}}$ ,  
321 likely corresponding to the extent of  $\Delta S_{10 \text{ ppb O}_3} / S_0$  that can be explained by surface reservoir  
322 effects. This interpretation is supported by two observations. Firstly, the data points generally  
323 are aligned with expected stickiness of parent compounds. Specifically, the lowest five points  
324 correspond to relatively high volatility species —  $\text{C}_3\text{H}_4\text{N}^+$ ,  $\text{C}_5\text{H}_5\text{O}_2^+$ ,  $\text{C}_3\text{H}_5\text{O}^+$ ,  $\text{CH}_3\text{O}^+$ , and  
325  $\text{CH}_5\text{O}^+$  — whereas the highest five are for species with lower volatility —  $\text{C}_{15}\text{H}_{27}\text{N}_2^+$ ,  $\text{C}_9\text{H}_{15}\text{O}_2^+$ ,  
326  $\text{C}_7\text{H}_{11}\text{O}^+$ ,  $\text{C}_{15}\text{H}_{23}^+$ , and  $\text{C}_8\text{H}_{17}\text{O}_2^+$ . Secondly, all values of  $C_{1 \text{ h}^{-1}} / C_{0.25 \text{ h}^{-1}}$  on the line are less than  
327 1.0 (solid line), consistent with expectation from a surface reservoir effect, which can make  
328 indoor species concentration at the higher air change rate close to, but no more than (dotted line),  
329 that at the lower air change rate.

330 Based on the above analysis, we can consider that the VOC signals for points situated  
331 well above the line in Fig. 5 are strongly produced by ozone chemistry. Among these VOC  
332 signals,  $\text{C}_8\text{H}_{15}\text{O}^+$  and  $\text{C}_8\text{H}_{13}^+$  attributed to 6-MHO exhibited a notably high  $\Delta S_{10 \text{ ppb O}_3} / S_0$  value  
333 above 20. Other VOC signals well above the line (i.e., above the grey region) include  $\text{C}_5\text{H}_9\text{O}_2^+$   
334 attributable to 4-OPA,  $\text{C}_9\text{H}_{17}\text{O}^+$  and  $\text{C}_9\text{H}_{15}^+$  attributable to nonenal, and ions attributable to the  
335  $\text{C}_8\text{-C}_{12}$  saturated aldehydes. As presented in Table 1, the total effective yield for all identified  
336 compounds is at least 12%. The effective yield of nonenal was the highest ( $\geq 3.5\%$ ), followed by  
337 6-MHO (2.7%), 4-OPA (2.6%), decanal ( $\geq 1.3\%$ ), and nonenal ( $\geq 1.0\%$ ). Note that, except for  
338 6-MHO and 4-OPA, the estimated yields represent lower limits, since our analysis might have  
339 missed some smaller fragment ions of these aldehydes (SI Appendix). The identified compounds,  
340 with summed indoor concentration of several ppb, contribute only marginally to the total loading

341 of oxygenated VOCs in this house, which was several hundred ppb (24). However, certain  
342 products may contribute even at low abundances to odors (e.g., nonenal (41)) or irritation (e.g.,  
343 4-OPA (42)).

344 Volatile products identified through this non-target analysis are among the most  
345 commonly reported products from ozone interaction with indoor surfaces and human skin oil.  
346 The C8-C10 aldehydes, particularly nonenal, have been reported as key products of ozonolysis  
347 for many indoor building and furnishing materials (9–11, 15). Surface soiling by oleic  
348 acids/esters from cooking oil might lead to additional nonenal production, as suggested by field  
349 measurements (8, 16), as well as by lab tests of building materials placed in real indoor  
350 environments (17). Notably, Wang and Morrison found that nonenal was the most prominent  
351 secondary aldehyde emitted from almost all the tested surfaces in residences they studied (8, 16);  
352 the product yield varied in the range 0-34% across the surfaces sampled. Their observation is  
353 consistent with our finding that nonenal exhibited the highest effective yield of  $\geq 3.5\%$  among all  
354 identified products. For ozone interaction with skin lipids, decanal is another key oxidation  
355 product in addition to 6-MHO and 4-OPA, specifically from ozonolysis of some abundant  
356 unsaturated fatty acids such as cis-hexadec-6-enoic acid (5-6% of skin surface lipids by weight)  
357 (18). In terms of relative ratios, yields of the three compounds quantified herein (2.7% (6-  
358 MHO):2.6% (4-OPA): $\geq 1.3\%$  (decanal)), were comparable with those reported in a simulated  
359 office experiment for skin oil ozonolysis with two occupants (14.4% (6-MHO):12.5% (4-  
360 OPA):6.3% (decanal)) (14). Octanal, undecanal, and dodecanal were also detected in skin oil  
361 ozonolysis experiments, but their fatty acid precursors are less abundant (14).

362 The unsaturated aldehyde nonenal has been previously identified as an oxidation product  
363 of new carpets (2-nonenal) (11, 16), certain skin surface lipids (3-nonenal) (18), omega-7  
364 unsaturated fatty acids (2-nonenal) (43), and linoleic acid (2- and 4- nonenal) (44), a common

365 constituent of linseed oil and certain cooking oils. In the house we studied, there were older area  
366 carpets in several rooms, and cooking activities occurred frequently. We cannot glean from the  
367 evidence which precursor(s) contributed to the secondary production of nonenal. Worth noting  
368 is that nonenal was not detected in previous field measurements on kitchen countertops where  
369 nonanal was prominent (8, 16). However, we suspect that result might be a technical artifact  
370 arising from the off-line analysis method used in those studies. That is, nonenal, which contains  
371 a C=C bond, might have been consumed by ozone reaction after collection on Tenax tubes,  
372 considering the use of a high level of ozone (40-120 ppb) and the absence of an ozone scrubber  
373 during sampling. In any case, given the high yield of nonenal observed here, in combination  
374 with the particularly low odor threshold for this compound (41), further investigation of nonenal  
375 from indoor ozonolysis reactions is warranted.

376         It should be noted that some frequently reported ozonolysis products in previous studies  
377 of indoor surfaces or skin oil, including formaldehyde, acetone, hexanal, and geranylacetone, did  
378 not emerge as apparent ozone byproducts in our analysis (Fig. 5). Ions corresponding to  
379 formaldehyde ( $\text{CH}_3\text{O}^+$ ) and hexanal ( $\text{C}_6\text{H}_{13}\text{O}^+$ ) lie near the baseline in Fig. 5, suggesting no more  
380 than a marginal contribution of ozone chemistry to indoor formaldehyde and hexanal generation.  
381 Major indoor sources of formaldehyde include urea-formaldehyde-bonded composite wood  
382 products (45). Continuous indoor sources of hexanal are uncertain, but may be related to certain  
383 wood materials (46, 47). Acetone was excluded from the analysis in Figure 5, because of strong  
384 contributions from intermittent sources as indicated by a high mean-to-median concentration  
385 ratio (24). Sources of acetone include human breath and household cleaning agents. The yield of  
386 acetone has been reported to be about 2 times higher than 6-MHO for skin oil ozonolysis (14),  
387 but the measured indoor concentration of acetone in the present study was 50 times higher than  
388 of 6-MHO, suggesting that the contribution of ozone chemistry for acetone at this site was

389 relatively small. Geranylacetone was also excluded in Figure 5, because its indoor-to-outdoor  
390 ratio (indicator for strong indoor source) and mean-to-median ratio did not reach the selection  
391 criteria. Even if we relax the data constraint to include the product ion of geranylacetone in the  
392 analysis (Figure S4), the ion lies in the grey region and is characterized by a high value of  $C_{1\text{ h}^{-1}} /$   
393  $C_{0.25\text{ h}^{-1}}$ . A probable interpretation is that the stickiness of geranylacetone to indoor surfaces  
394 strongly interferes with our ability to discern its relationship to ozone-initiated chemistry using  
395 our approach. Given the presence of these and other compounds which can be contributed by  
396 ozone chemistry but did not emerge as apparent ozone byproducts, the actual total yield of  
397 volatile organic products from ozone chemistry in the house can be several times higher than the  
398 summed effective yield of all identified compounds reported here.

399 To summarize, the results presented in this paper represent the first quantitative  
400 characterization of ozone-initiated chemistry in a normally occupied residence. We identified a  
401 range of VOCs that had strong contributions from indoor ozone chemistry (Fig. 5), even though  
402 the house we studied had both low indoor ozone concentrations (Fig. 1) and a low indoor ozone  
403 loss rate (Fig. 2). Being able to elucidate how residential VOC composition is altered by ozone-  
404 initiated chemistry substantiates prior laboratory-based investigations. It is important to  
405 recognize that the health effects associated with ambient ozone might be materially influenced  
406 by the products of indoor ozone chemistry. Of concern in this regard are not only those species  
407 characterized here, but also other potentially toxic products known to be a consequence of  
408 ozonolysis, but which our instrumentation is incapable of detecting, such as secondary ozonides,  
409 hydroperoxides, and epoxides (48, 49).

410

## 411 **Materials and Methods**

412 The studied house, built in the 1930s of wood-frame construction, has a split-level living  
413 zone, an unoccupied attic above, and a small basement and larger crawlspace below. Two adult  
414 occupants (male and female, aged 60-65 y) live in the house. In addition to normal house  
415 operation conditions (occupied periods), the occupants were deliberately away on a few  
416 occasions for one or more days during the monitoring period. During the vacant periods, the  
417 house windows and exterior doors were closed. Other than a request to maintain interior doors  
418 open (to facilitate interzonal transport and mixing), occupants were instructed to live as they  
419 normally would, including normal use of window opening to maintain thermal comfort. The  
420 occupants gave informed consent for this study, which was approved by the Committee for  
421 Protection of Human Subjects for the University of California, Berkeley (Protocol #2016-04-  
422 8656).

423 Ozone and VOCs were measured using a UV-absorption based ozone monitor (Thermal  
424 49i) and a PTR-ToF-MS, respectively. Both instruments were situated in a detached garage and  
425 sub-sampled via shared continuous-operating equal length 30-meter PFA sampling lines from the  
426 kitchen, bedroom, crawlspace, basement, attic, and outdoors. During vacant periods, sampling  
427 was conducted using a spaced-resolved scheme (sampling from each of the 6 locations for 5  
428 mins in a twice-per-hour cycle). During occupied periods, sampling was conducted using the  
429 space-resolved measurement scheme for ~ 5 weeks and using a time-resolved scheme (outdoor 5  
430 mins, kitchen 20 mins, and bedroom 5 mins, twice per hour) for ~ 2 weeks. SI Appendix  
431 provides a detailed description of the sampling system, associated data trimming protocols, as  
432 well as an evaluation of the influence of the sampling system on instrument response.

433 For PTR-ToF-MS, the primary reagent is the hydronium ion ( $\text{H}_3\text{O}^+$ ), which can  
434 effectively protonate most oxygenated VOCs. Resultant product ions were measured, often in  
435 the form of  $\text{VOCH}^+$ , but fragmentation can also occur. In total, 218 VOC signals (organic ion

436 formulas after combining isotopic ions and some known fragment ions) were extracted to  
437 represent measured VOC speciation across the campaign (24). Depending on sample air  
438 composition, a VOC signal might be dominantly attributed to one VOC species, and might be  
439 contributed by a few species. Airborne concentrations (in part per trillion/billion by volume,  
440 ppt/ppb) were estimated for individual VOC signals as described in SI Appendix.

441 Data associated with this paper is provided in Dataset S1.

**Acknowledgments.** This work was funded by the Alfred P. Sloan Foundation via Grants 2016-7050 and 2019-11412. Y. J. Liu acknowledges support from Alfred P. Sloan Foundation MoBE Postdoctoral Fellowship (Grant 2015-14166) and support by the 111 Project (Grant B20009). We thank occupants in the studied house for volunteering their house and facilitating the measurements. We thank Jianyin Xiong, Yilin Tian, and Robin Weber for their contribution to the field campaign.

**Author contribution.** A.G., W.N., Y.L., P.M., and C.A. designed the field campaign, Y.L., P.M., and C.A. collected the PTR-ToF-MS and ozone data, Y.L., C.W., W.N., and A.G. analyzed the data, Y.L. wrote the manuscript, and all authors edited the manuscript and provided comments.

## **ORCID**

Yingjun Liu <https://orcid.org/0000-0001-6659-3660>

Pawel K. Misztal <https://orcid.org/0000-0003-1060-1750>

Caleb Arata <https://orcid.org/0000-0002-0170-8794>

Charles J. Weschler <https://orcid.org/0000-0002-9097-5850>

William W. Nazaroff <https://orcid.org/0000-0001-5645-3357>

Allen H. Goldstein <https://orcid.org/0000-0003-4014-4896>

## References

1. M. Yao, B. Zhao, Surface removal rate of ozone in residences in China. *Build. Environ.* **142**, 101–106 (2018).
2. K. Lee, J. Vallarino, T. Dumyahn, H. Özkaynak, J. D. Spengler, Ozone decay rates in residences. *J. Air Waste Manage. Assoc.* **49**, 1238–1244 (1999).
3. C. J. Weschler, Ozone’s impact on public health: contributions from indoor exposures to ozone and products of ozone-Initiated chemistry. *Environ. Health Perspect.* **114**, 1489–1496 (2006).
4. B. L. Deming, P. J. Ziemann, Quantification of alkenes on indoor surfaces and implications for chemical sources and sinks. *Indoor Air* **30**, 914–924 (2020).
5. J. Shen, Z. Gao, Ozone removal on building material surface: A literature review. *Build. Environ.* **134**, 205–217 (2018).
6. C. J. Weschler, Ozone in indoor environments: Concentration and chemistry. *Indoor Air* **10**, 269–288 (2000).
7. C. Chen, B. Zhao, C. J. Weschler, Assessing the influence of indoor exposure to “outdoor ozone” on the relationship between ozone and short-term mortality in U.S. communities. *Environ. Health Perspect.* **120**, 235–240 (2012).
8. H. Wang, G. Morrison, Ozone-surface reactions in five homes: surface reaction probabilities, aldehyde yields, and trends. *Indoor Air* **20**, 224–234 (2010).
9. M. Nicolas, O. Ramalho, F. Maupetit, Reactions between ozone and building products: Impact on primary and secondary emissions. *Atmos. Environ.* **41**, 3129–3138 (2007).



10. S. P. Lamble, R. L. Corsi, G. C. Morrison, Ozone deposition velocities, reaction probabilities and product yields for green building materials. *Atmos. Environ.* **45**, 6965–6972 (2011).
11. G. C. Morrison, W. W. Nazaroff, Ozone interactions with carpet: Secondary emissions of aldehydes. *Environ. Sci. Technol.* **36**, 2185–2192 (2002).
12. L. S. Pandrangi, G. C. Morrison, Ozone interactions with human hair: Ozone uptake rates and product formation. *Atmos. Environ.* **42**, 5079–5089 (2008).
13. B. K. Coleman, H. Destailats, A. T. Hodgson, W. W. Nazaroff, Ozone consumption and volatile byproduct formation from surface reactions with aircraft cabin materials and clothing fabrics. *Atmos. Environ.* **42**, 642–654 (2008).
14. A. Wisthaler, C. J. Weschler, Reactions of ozone with human skin lipids: Sources of carbonyls, dicarbonyls, and hydroxycarbonyls in indoor air. *Proc. Natl. Acad. Sci.* **107**, 6568–6575 (2010).
15. O. A. Abbass, D. J. Sailor, E. T. Gall, Effect of fiber material on ozone removal and carbonyl production from carpets. *Atmos. Environ.* **148**, 42–48 (2017).
16. H. Wang, G. C. Morrison, Ozone-initiated secondary emission rates of aldehydes from indoor surfaces in four homes. *Environ. Sci. Technol.* **40**, 5263–5268 (2006).
17. C. J. Cros, G. C. Morrison, J. A. Siegel, R. L. Corsi, Long-term performance of passive materials for removal of ozone from indoor air. *Indoor Air* **22**, 43–53 (2012).
18. C. J. Weschler, Roles of the human occupant in indoor chemistry. *Indoor Air* **26**, 6–24 (2016).
19. M. Kruza, A. C. Lewis, G. C. Morrison, N. Carslaw, Impact of surface ozone interactions on indoor air chemistry: A modeling study. *Indoor Air* **27**, 1001–1011 (2017).

20. P. Wolkoff, Volatile organic compounds - Sources, measurements, emissions, and the impact on indoor air quality. *Indoor Air* **5 (Suppl. 3)**, 9–73 (1995).
21. J. Xiong, Z. He, X. Tang, P. K. Misztal, A. H. Goldstein, Modeling the time-dependent concentrations of primary and secondary reaction products of ozone with squalene in a university classroom. *Environ. Sci. Technol.* **53**, 8262–8270 (2019).
22. C. J. Weschler, *et al.*, Ozone-initiated chemistry in an occupied simulated aircraft cabin. *Environ. Sci. Technol.* **41**, 6177–6184 (2007).
23. A. Fischer, E. Ljungström, S. Langer, Ozone removal by occupants in a classroom. *Atmos. Environ.* **81**, 11–17 (2013).
24. Y. Liu, *et al.*, Characterizing sources and emissions of volatile organic compounds in a northern California residence using space- and time-resolved measurements. *Indoor Air* **29**, 630–644 (2019).
25. Y. Liu, *et al.*, Detailed investigation of ventilation rates and airflow patterns in a northern California residence. *Indoor Air* **28**, 572–584 (2018).
26. C. Arata, *et al.*, Measurement of NO<sub>3</sub> and N<sub>2</sub>O<sub>5</sub> in a residential kitchen. *Environ. Sci. Technol. Lett.* **5**, 595–599 (2018).
27. K. Lee, *et al.*, Nitrous acid, nitrogen dioxide, and ozone concentrations in residential environments. *Environ. Health Perspect.* **110**, 145–149 (2002).
28. H. Zhao, B. Stephens, A method to measure the ozone penetration factor in residences under infiltration conditions: application in a multifamily apartment unit. *Indoor Air* **26**, 571–581 (2016).
29. C. M. Salvador, *et al.*, Indoor ozone/human chemistry and ventilation strategies. *Indoor Air* **29**, 913–925 (2019).

30. E. Grosjean, D. Grosjean, J. H. Seinfeld, Gas-phase reaction of ozone with trans-2-hexenal, trans-2-hexenyl acetate, ethylvinyl ketone, and 6-methyl-5-hepten-2-one. *Int. J. Chem. Kinet.* **28**, 373–382 (1996).
31. C. J. Weschler, W. W. Nazaroff, Growth of organic films on indoor surfaces. *Indoor Air* **27**, 1101–1112 (2017).
32. E. T. Gall, D. Rim, Mass accretion and ozone reactivity of idealized indoor surfaces in mechanically or naturally ventilated indoor environments. *Build. Environ.* **138**, 89–97 (2018).
33. C.-Y. Huo, *et al.*, Phthalate esters in indoor window films in a northeastern Chinese urban center: Film growth and implications for human exposure. *Environ. Sci. Technol.* **50**, 7743–7751 (2016).
34. C. Y. Lim, J. P. Abbatt, Chemical composition, spatial homogeneity, and growth of indoor surface films. *Environ. Sci. Technol.* **54**, 14372–14379 (2020).
35. C. J. Weschler, *et al.*, Squalene and cholesterol in dust from Danish homes and daycare centers. *Environ. Sci. Technol.* **45**, 3872–3879 (2011).
36. H. Baker, A. M. Kligman, Technique for estimating turnover time of human stratum corneum. *Arch. Dermatol.* **95**, 408–411 (1967).
37. A. Zafar, J. Chickos, The vapor pressure and vaporization enthalpy of squalene and squalane by correlation gas chromatography. *J. Chem. Thermodyn.* **135**, 192–197 (2019).
38. X. Tang, P. K. Misztal, W. W. Nazaroff, A. H. Goldstein, Volatile organic compound emissions from humans indoors. *Environ. Sci. Technol.* **50**, 12686–12694 (2016).
39. C. Fortenberry, *et al.*, Analysis of indoor particles and gases and their evolution with natural ventilation. *Indoor Air* **29**, 761–779 (2019).

40. C. Wang, *et al.*, Surface reservoirs dominate dynamic gas-surface partitioning of many indoor air constituents. *Sci. Adv.* **6**, eaay8973 (2020).
41. D. G. Guadagni, R. G. Buttery, S. Okano, Odour thresholds of some organic compounds associated with food flavours. *J. Sci. Food Agric.* **14**, 761–765 (1963).
42. S. E. Anderson, *et al.*, Irritancy and allergic responses induced by exposure to the indoor air chemical 4-oxopentanal. *Toxicol. Sci.* **127**, 371–381 (2012).
43. S. Haze, *et al.*, 2-Nonenal newly found in human body odor tends to increase with aging. *J. Invest. Dermatol.* **116**, 520–524 (2001).
44. T. Moise, Y. Rudich, Reactive uptake of ozone by aerosol-associated unsaturated fatty acids: Kinetics, mechanism, and products. *J. Phys. Chem. A* **106**, 6469–6476 (2002).
45. T. Salthammer, S. Mentese, R. Marutzky, Formaldehyde in the indoor environment. *Chem. Rev.* **110**, 2536–2572 (2010).
46. A.-M. Manninen, P. Pasanen, J. K. Holopainen, Comparing the VOC emissions between air-dried and heat-treated Scots pine wood. *Atmos. Environ.* **36**, 1763–1768 (2002).
47. A. T. Hodgson, A. F. Rudd, D. Beal, S. Chandra, Volatile organic compound concentrations and emission rates in new manufactured and site-built houses. *Indoor Air* **10**, 178–192 (2000).
48. S. Zhou, M. W. Forbes, J. P. D. Abbatt, Kinetics and products from heterogeneous oxidation of squalene with ozone. *Environ. Sci. Technol.* **50**, 11688–11697 (2016).
49. M. Yao, C. J. Weschler, B. Zhao, L. Zhang, R. Ma, Breathing-rate adjusted population exposure to ozone and its oxidation products in 333 cities in China. *Environ. Int.* **138**, 105617 (2020).

## List of Figures

**Figure 1.** Diel variation of (top) ozone concentrations in various locations of the studied house, (middle) indoor ozone concentration in the living space normalized by outdoor concentration ( $I/O$ ), and (bottom) apportionment of air flowing into the living space, between directly from outdoors and via the crawlspace. Data are shown for normally occupied period averaged during the five-week-long space-resolved measurement mode. The solid lines, respectively, represent medians; the shaded regions represent the corresponding interquartile ranges.

**Figure 2.** Scatter plot of the indoor chemical loss rates of ozone  $L_{O_3}$  (ppb/h) versus the living-space ozone concentration  $[O_3]_{in}$  (ppb). The loss rate,  $L_{O_3}$ , was calculated using Eq. 2 based on the mass balance of ozone in the living space with 2-h resolution. Data are shown for times when the outdoor fraction of total airflow into the living space ( $f_{out}$ ) is greater than 0.6. The solid orange line represents the best linear fit to the data. Dashed orange lines have slopes of 0.8 and 2.0  $h^{-1}$ , respectively.

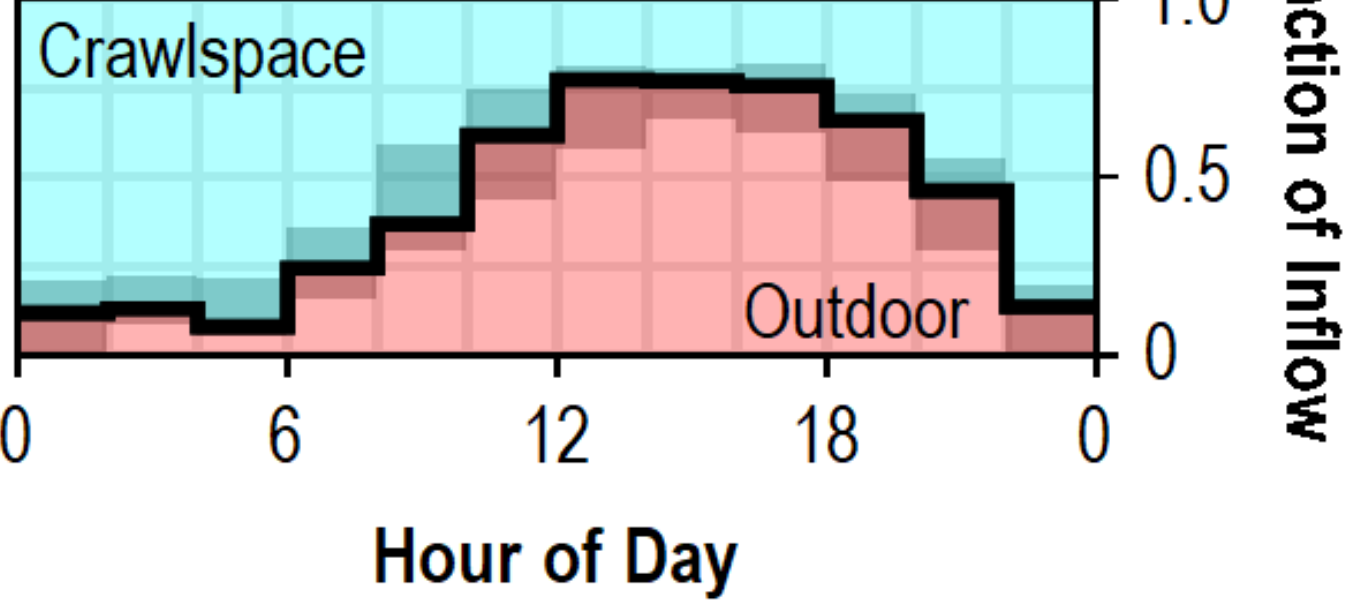
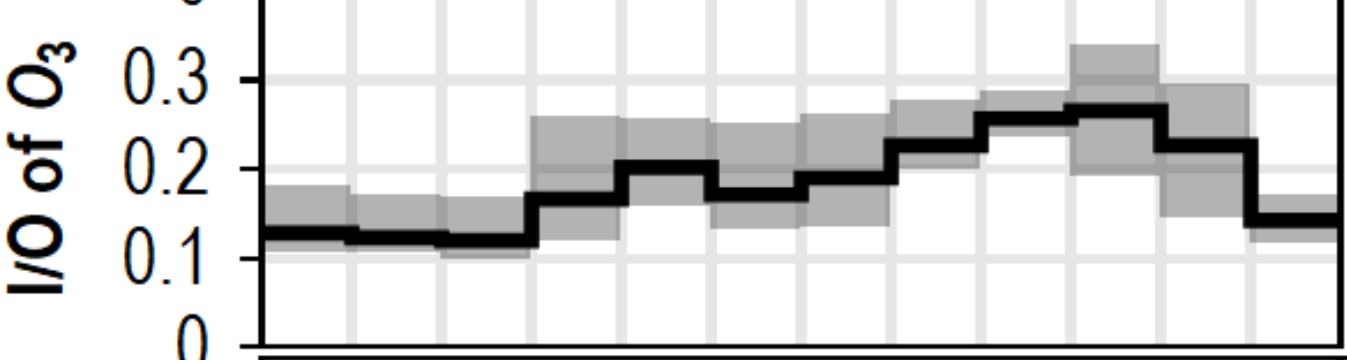
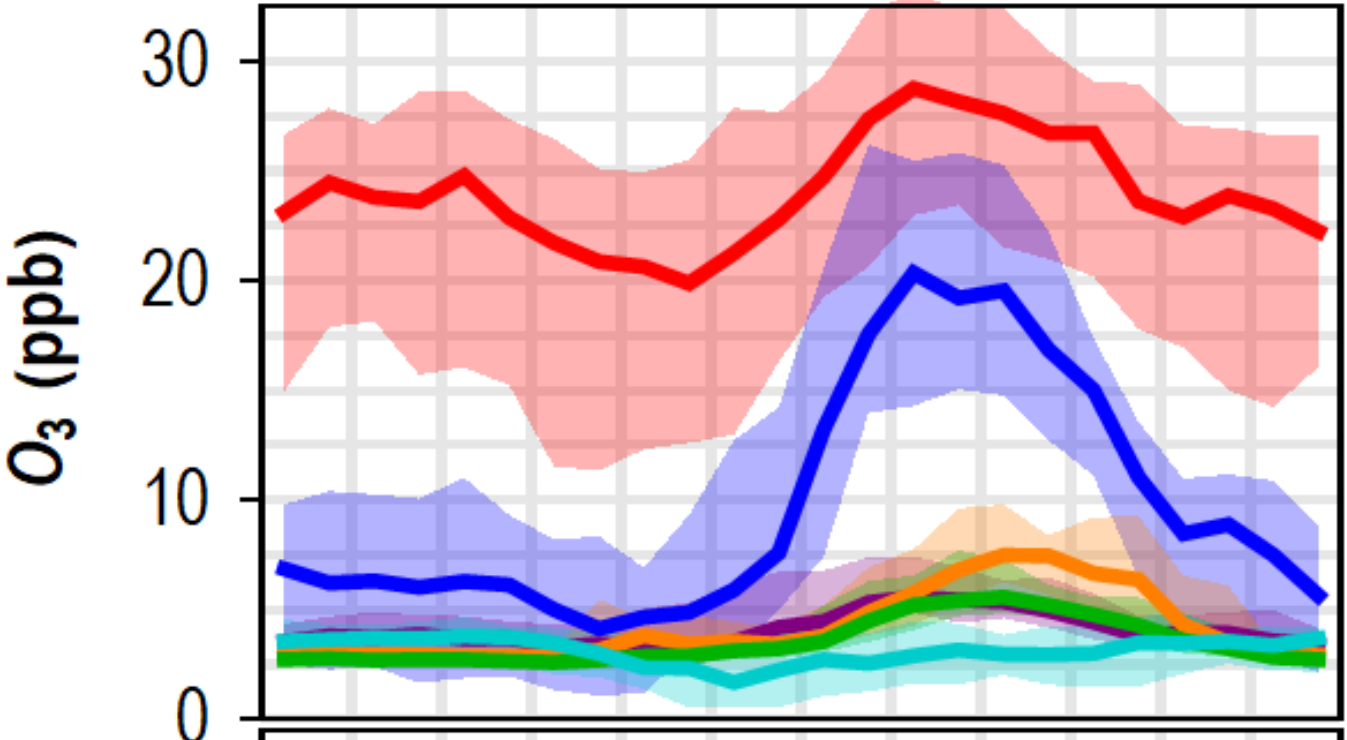
**Figure 3.** Time series of VOC signals that might be attributed to products from squalene ozonolysis and possible influencing factors. Panels from top to bottom show occupancy (number of persons present indoors), air change rate (ACR;  $h^{-1}$ ), indoor temperature ( $T$ ;  $^{\circ}C$ ), ozone concentration (ppb),  $C_8H_{15}O^+$  signal (ppb), and  $C_5H_9O_2^+$  signal (ppb).  $C_8H_{15}O^+$  and  $C_5H_9O_2^+$  ions correspond to the protonated ions of 6-MHO ( $C_8H_{14}O$ ) and 4-OPA ( $C_5H_8O_2$ ) without fragmentation, respectively.

**Figure 4.** Dependence of  $C_8H_{15}O^+$  (6-MHO) source strength on (A) indoor ozone concentration and (B) occupancy. Panel A shows all available data using 2-h resolution and restricted to an indoor temperature range of 20.5-23.5  $^{\circ}C$ . Panel B uses a subset of

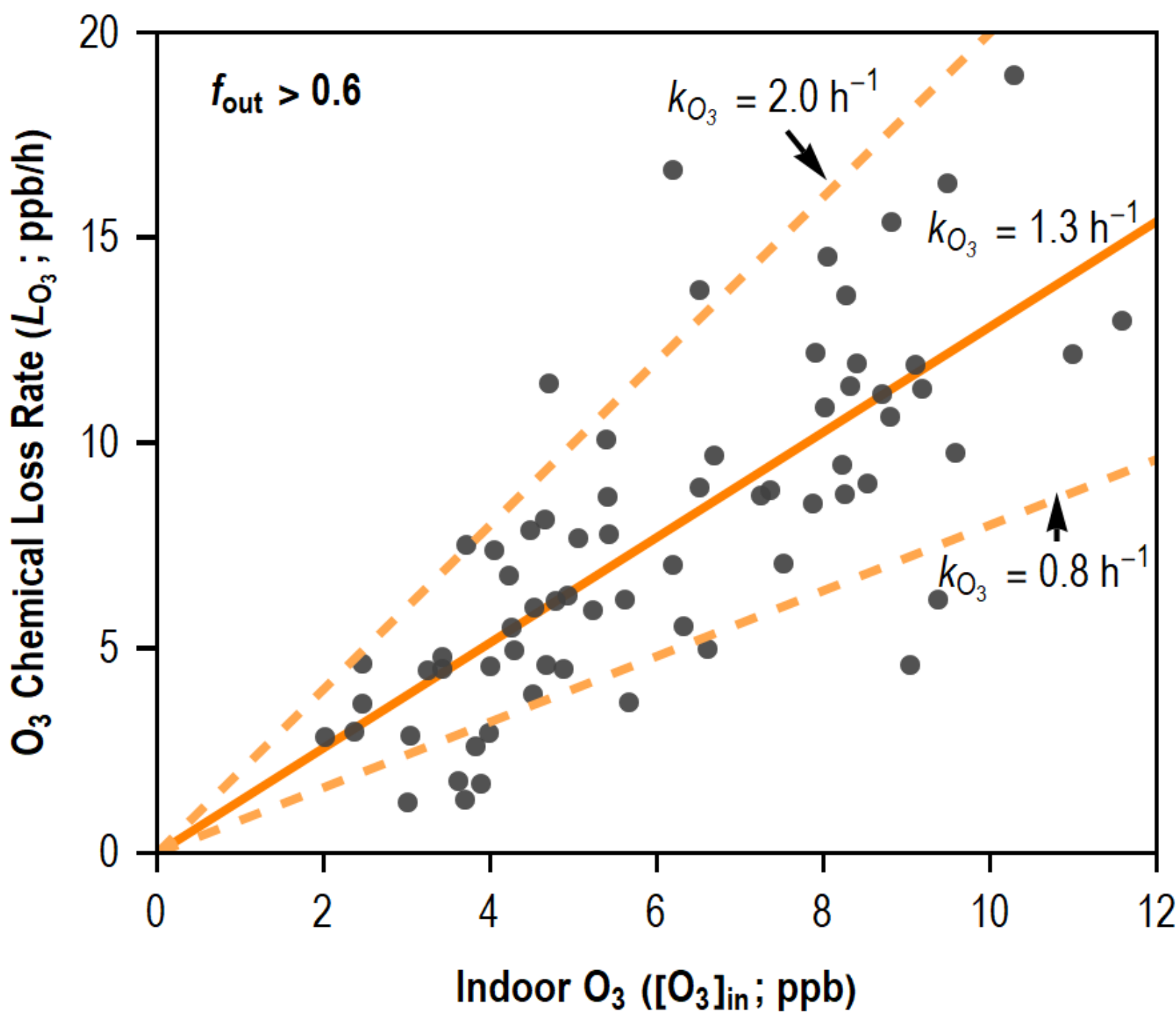
data in panel A (bounded by dashed lines, with indoor ozone of 2-4 ppb) and plots  $C_8H_{15}O^+$  source strength versus occupancy for  $2 \geq \text{occupancy} > 0$  (left side) and versus unoccupied time duration for occupancy = 0 (right side), respectively. Data points are colored to indicate occupancy level. In Panel A, the black line shows a linear fit of data after excluding outliers of  $C_8H_{15}O^+$  source strength ( $UQ + 3 \text{ IQR}$ ); exact occupancy level was labeled for occupancy  $> 4$ . Occupancy level represents the average for the 2-h integration period, and so can be a non-integer value when occupants are present for only part of the interval.

**Figure 5.** VOC signals for continuously emitted species mapped into a 2-dimensional plot to identify compounds with pronounced production from indoor ozone chemistry. The y axis is indoor source strength ratio, defined as change of source strength associated with a 10-ppb increase of ozone, normalized by the ozone-independent source strength ( $\Delta S_{10 \text{ ppb } O_3} / S_0$ ); and the x axis is an indoor concentration ratio, defined as concentration at an air change rate of  $1 \text{ h}^{-1}$  divided by that at  $0.25 \text{ h}^{-1}$  ( $C_{1 \text{ h}^{-1}} / C_{0.25 \text{ h}^{-1}}$ ). Each data point is colored by  $R^2$  of the linear fit of indoor source strength versus indoor ozone, and the point size is scaled to the corresponding slope ( $k$ ). The grey line represents a fit to the baseline. Emissions for chemicals along this line are ozone independent. The light grey region represents an approximate uncertainty band, plotted as the line value  $\pm 1$ .

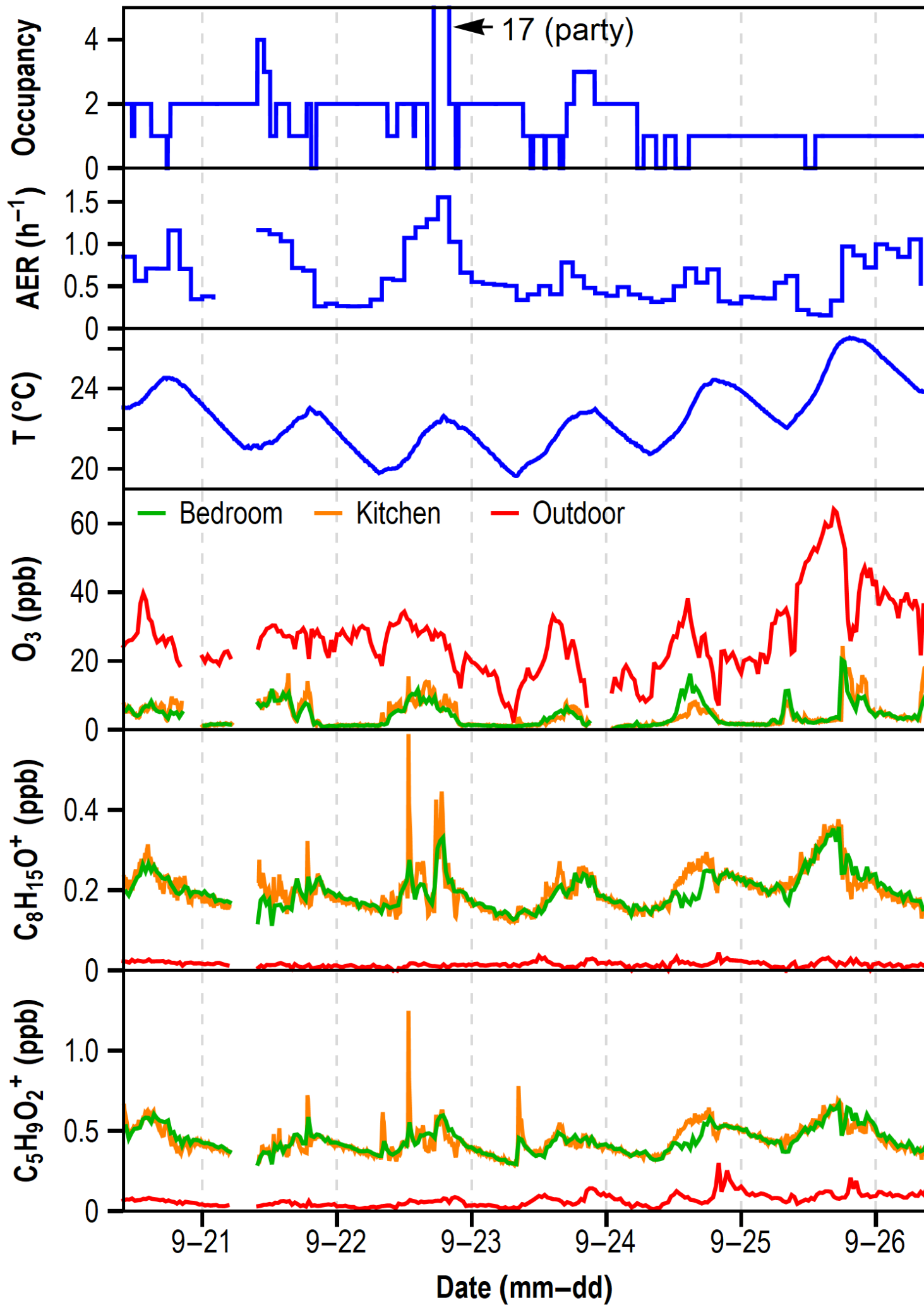
- Attic
- Bedroom
- Kitchen
- Basement
- Crawlspace
- Outdoor

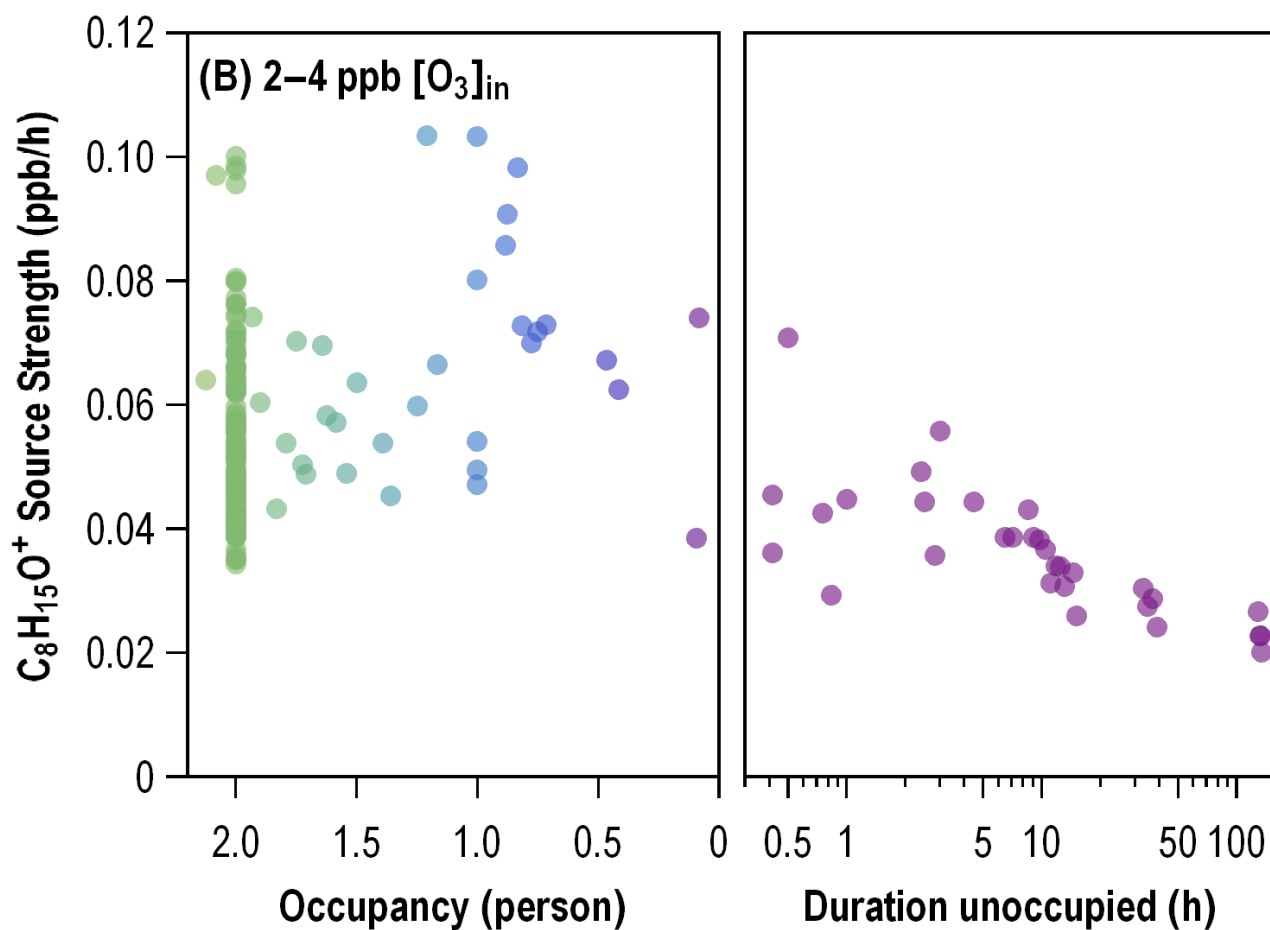
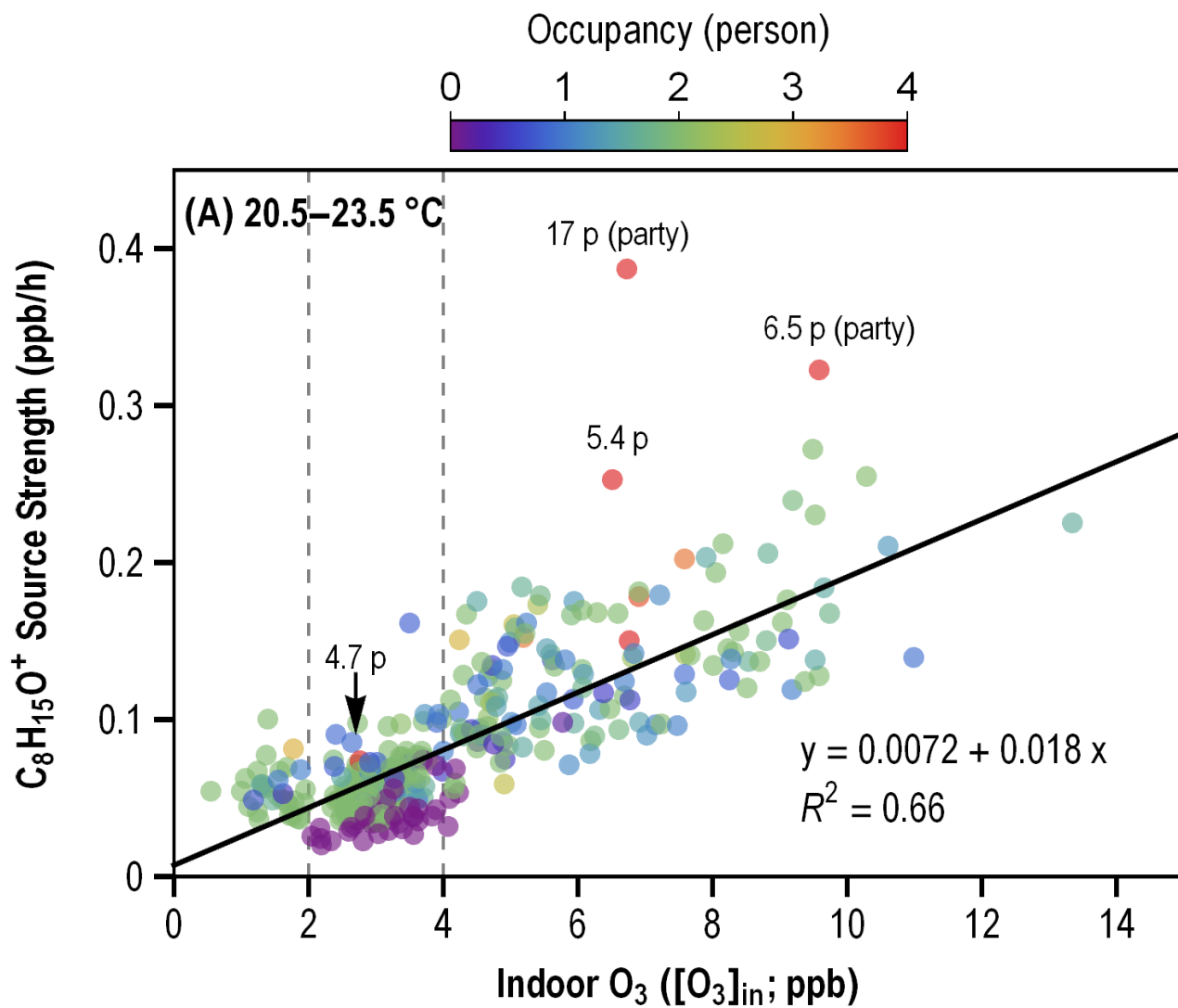


**Hour of Day**









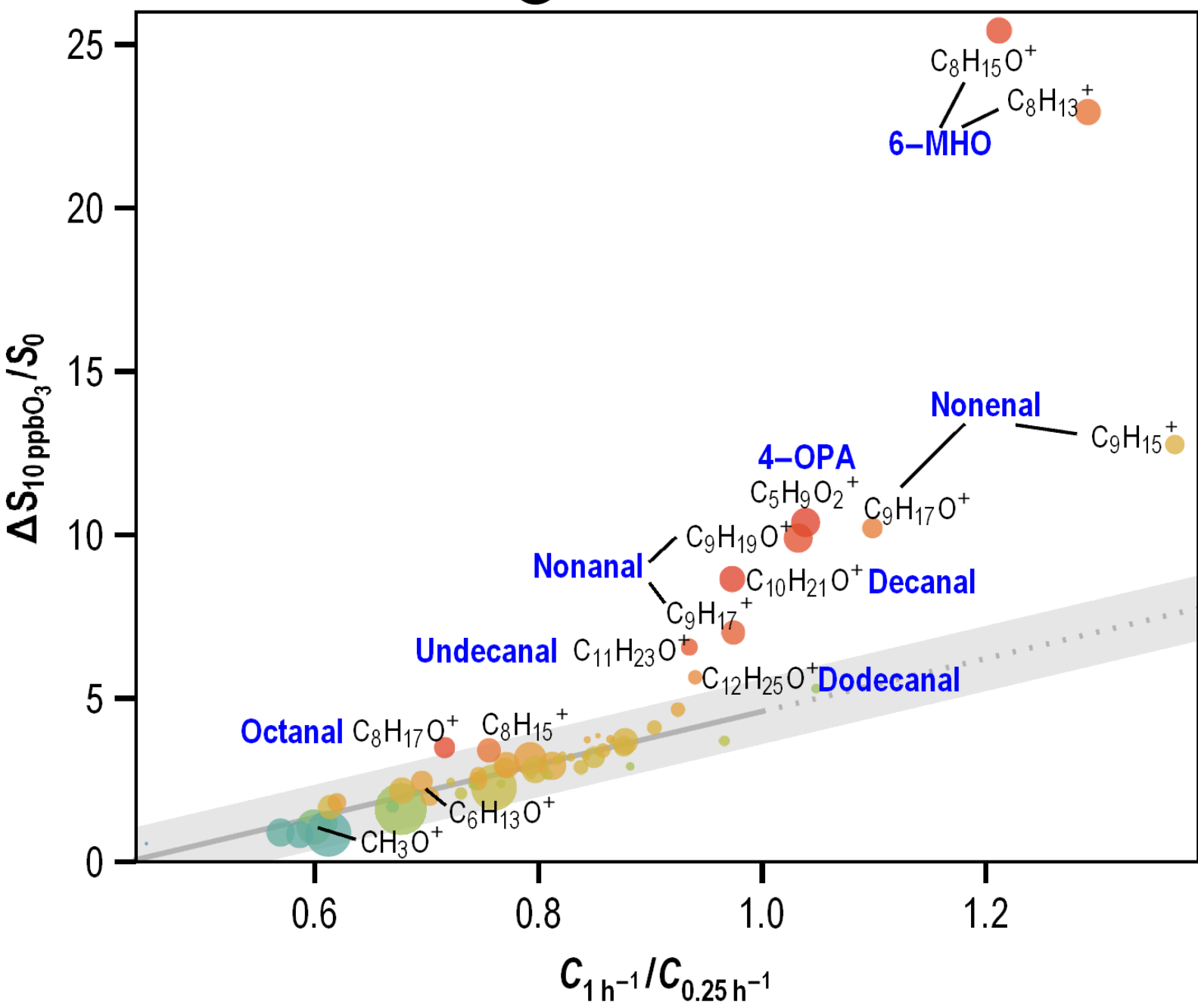
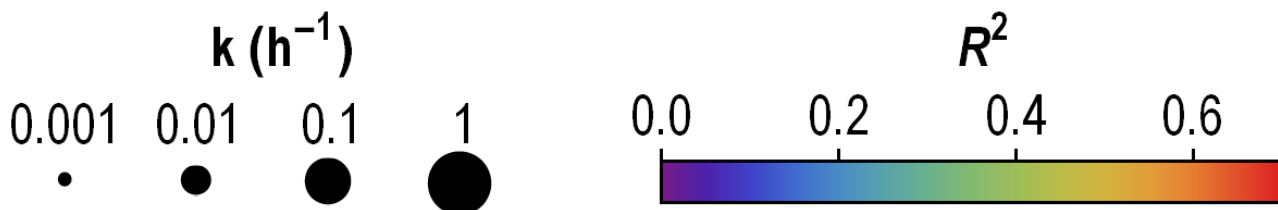


**Table 1** Summary for ozone concentration and VOC signals identified as having a major origin from indoor ozone chemistry.

VOC signals		Mean mixing ratio <sup>d</sup> (ozone in ppb; VOC signals in ppt)						Derived parameters <sup>e</sup>				
Ion <sup>a</sup>	Species <sup>b</sup>	Outdoor	Kitchen	Bedroom	Crawlspace	Basement	Attic	$k$ (h <sup>-1</sup> )	$\Delta S_{10 \text{ ppb } O_3}/S_0$	$C_{1 \text{ h}^{-1}}/C_{0.25 \text{ h}^{-1}}$	Yield <sup>f</sup>	
Ozone		23	4.6	3.8	3.4	9.9	4.5					
PTR	C <sub>5</sub> H <sub>9</sub> O <sub>2</sub> <sup>+</sup>	4-OPA	39	400	420	56	190	240	0.034	10	1.04	2.6%
	C <sub>8</sub> H <sub>15</sub> O <sup>+</sup>	6-MHO	6	180	190	17	58	94	0.018	26	1.21	2.7%
	C <sub>8</sub> H <sub>13</sub> <sup>+</sup>	6-MHO <sup>c</sup>	7	160	170	19	59	100	0.016	23	1.29	
	C <sub>8</sub> H <sub>17</sub> O <sup>+</sup>	Octanal	4	120	130	12	31	77	0.008	3.6	0.72	≥0.6%
	C <sub>9</sub> H <sub>17</sub> O <sup>+</sup>	Nonenal	4	82	85	9	24	44	0.007	10	1.10	≥1.0%
	C <sub>9</sub> H <sub>15</sub> <sup>+</sup>	Nonenal <sup>c</sup>	5	71	65	9	25	30	0.006	13	1.37	
	C <sub>9</sub> H <sub>19</sub> O <sup>+</sup>	Nonanal	3	370	370	21	98	160	0.033	10	1.03	≥3.5%
	C <sub>9</sub> H <sub>17</sub> <sup>+</sup>	Nonanal <sup>c</sup>	5	150	150	17	71	67	0.012	7.1	0.97	
	C <sub>10</sub> H <sub>21</sub> O <sup>+</sup>	Decanal	6	200	230	17	87	90	0.018	8.7	0.97	≥1.3%
	C <sub>11</sub> H <sub>23</sub> O <sup>+</sup>	Undecanal	3	45	52	6	20	26	0.004	6.6	0.93	≥0.3%
	C <sub>12</sub> H <sub>25</sub> O <sup>+</sup>	Dodecanal	2	28	32	5	13	15	0.002	5.7	0.94	≥0.2%

<sup>a</sup> The PTR ions presented here are those well above the baseline in Fig. 5.

<sup>b</sup> Species are attributed by matching identified ion formulas with known indoor ozonolysis products. These species probably make a dominant contribution to corresponding ion signals in the living space but may or may not in other spaces.

<sup>c</sup> Ratios of two VOC signals attributed to the same species might be slightly different in kitchen and bedroom due to the presence of other minor contributing species.

<sup>d</sup> Mean mixing ratio during occupied period when in space-resolved measurement mode.

<sup>e</sup> See detailed description of the parameters in the main text.

<sup>f</sup> Yield for identified VOC species, estimated as the sum of yields for respective identified product ions. For some species, the sum only represents a lower limit due to the possible presence of unidentified fragment ions (cf. SI Appendix).